Journal of Solid State Chemistry 184 (2011) 1251–1256

Contents lists available at ScienceDirect

Journal of Solid State Chemistry

journal homepage: www.elsevier.com/locate/jssc

Synthesis and structural analysis of $Bi_{2-y}Sr_yIr_2O_7$, a new pyrochlore solid solution

Carlos Cosio-Castaneda [a,*], Pablo de la Mora [b], Gustavo Tavizon [a]

[a] Departamento de Física y Química Teórica, Facultad de Química, Universidad Nacional Autónoma de México, Ciudad Universitaria, México, D.F. 04510, México
[b] Departamento de Física, Facultad de Ciencias, Universidad Nacional Autónoma de México, Ciudad Universitaria, México, D.F. 04510, México

ARTICLE INFO

Article history:
Received 29 July 2010
Received in revised form
2 December 2010
Accepted 1 March 2011
Available online 29 March 2011

Keywords:
Iridium pyrochlores
Rietveld analysis
Electrical resistivity

ABSTRACT

This paper presents a study of the synthesis and structural properties of the new pyrochlore-type $Bi_{2-y}Sr_yIr_2O_7$ series. Ten compositions with $0.0 \le y \le 0.9$ were prepared by solid-state reaction with thermal treatments at 873, 1073 and 1323 K under atmospheric pressure conditions. Structural refinements from X-ray powder diffraction data by the Rietveld method show that all compounds of the $Bi_{2-y}Sr_yIr_2O_7$ solid solution crystallize in a α-pyrochlore structure. The main structural difference when bismuth is substituted by strontium concerns the *x* position of the O1 (x, $^1/_8$, $^1/_8$). This substitution significantly increases the Bi/Sr–O1 distance and diminishes the Ir–O1 distance; this implies that the Ir–O1–Ir bond angle increases. With the Sr substitution, the IrO_6 local configuration goes from a flattened trigonal antiprism, $y < 0.5$, to an elongated one, $y > 0.5$, passing through an octahedral array, $y \sim 0.5$. The electrical consequences of these structural changes observed in this system are qualitatively explained with electronic structure calculations, this behavior agrees very well with those observed in other pyrochlore systems $A_2M_2O_7$ (A=rare earth cations or Tl^+, Pb^{2+}, or Bi^{3+}, and M=Ru or Ir).

1. Introduction

During the last decade, there has been substantial interest in the research of compounds crystallizing in the α-pyrochlore structure. This is mainly because they have important technological applications such as catalysis, compounds for nuclear waste immobilization, electronic systems, etc. [1–6], most of these applications are related with the flexibility with which chemical elements can be incorporated into the pyrochlore structure and to the remarkable high structure stability and response under high pressure and high radiation field [2,3]. Moreover, the α-pyrochlore-type magnetic compounds offer the possibility to analyze the complex magnetic phenomena exhibited by geometrically frustrated systems [7,8]. Additionally, some compounds crystallizing in this structure show sophisticated electrical properties such as superconductivity or insulator–metal Mott transitions [9,10]. Recently, from electronic structure calculations, a topological insulator character has been suggested for the $M_2Ir_2O_7$ system (M=Y or rare-earth element) [11]. The diverse chemistry of the pyrochlore structure and the remarkable variation of properties make this crystalline system one of the most versatile to study electric and magnetic phenomena in complex ceramic oxides.

Metal oxides with α-pyrochlore crystal structure are generally described with the general composition $A_2B_2O_7$ where A and B are generally tri- and tetravalent cations, respectively, although it is possible to find compounds with A^{2+} and B^{5+} [12]. The crystal structure of the α-pyrochlore, $A_2B_2O_7$, can be thought as consisting of two interpenetrating and independent networks, one of them is the anticristobalite-type and corresponds to the A_2O network; the other one is the B_2O_6 network in which B is in a distorted octahedral coordination (see Fig. 1). In both cases, there are corner-linked A_4 and B_4 tetrahedral networks that provide the possibility to have a highly frustrated magnetic moment interaction.

The Ir–Bi oxide based pyrochlore is highly susceptible of showing non-stoichiometry. This is the result of the high vapor pressure of both Bi_2O_3 and IrO_2 at the reaction temperature [13]. On the other hand, the deficiency of Bi in $Bi_2Ir_2O_7$ is associated with Bi surface segregation that forms an amorphous surface oxide [14].

Nowadays, there is special interest in α-pyrochlore $A_2Ir_2O_7$ iridiates. In this kind of compounds, when A^{3+} is a non-magnetic cation the magnetic properties are due to the tetravalent Ir only, which contains five 5*d* electrons in low spin S=½ configuration. This system with only one magnetic network could be thought as a reference system, in which magnetic frustration could appear

* Corresponding author.
E-mail address: carloscosioc@gmail.com (C. Cosio-Castaneda).

0022-4596/$ - see front matter © 2011 Elsevier Inc. All rights reserved.
doi:10.1016/j.jssc.2011.03.034

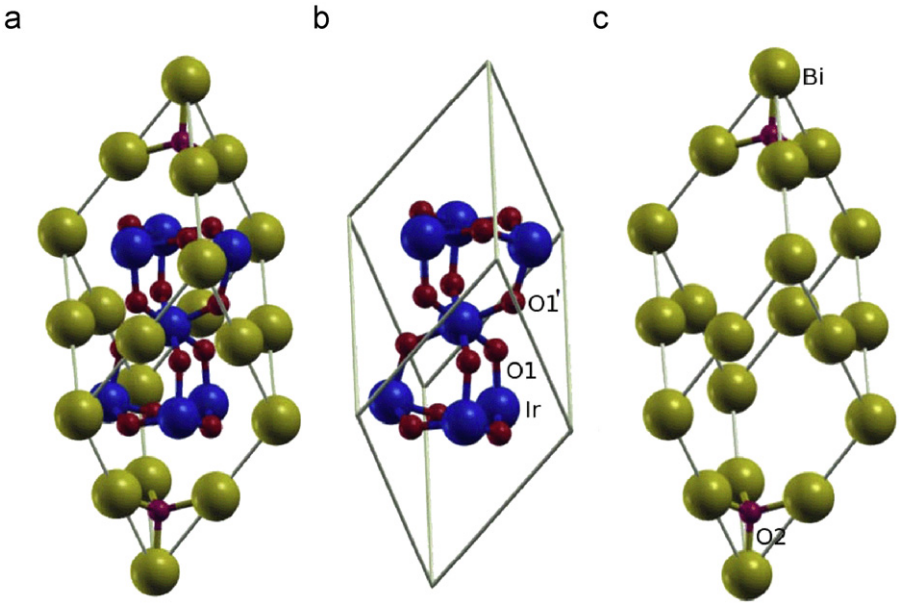

Fig. 1. Conventional unit cell of $Bi_2Ir_2O_7$ is a FCC cell. The primitive cell is trigonal (a) with 60° angles containing two formula units. The Ir atoms are arranged in a tetrahedral arrangement (b) each Ir is in two tetrahedron corners. These tetrahedra are arranged in a 3D diamond structure. There is an O1 atom outside each tetrahedron edge (Ir_2O_6). There are six O1 atoms around each Ir atom forming a distorted octahedron (see the central Ir in B), it can be a flattened or an elongated antiprism. Bi atoms have the same arrangement, but displaced by half cell (½, ½, ½) (c). In this case the oxygen, O2, is at the center of the tetrahedron (Bi_2O). Two Bi of one tetrahedron and two Ir of an adjacent tetrahedron form a Bi–Ir tetrahedron (Bi_2Ir_2O). There is an O1 atom inside, but displaced towards the Ir atoms. The positions of the atoms have been shifted by ½, ½, ½ for clarity.

[10]. For instance, the magnetic behavior of the $Y_2Ir_2O_7$ system could be described as that of a spin-glass with a small ferromagnetic component [15]. On the other hand, in some α-pyrochlore iridiates it is possible to explain the magnetic behavior as resulting from the localized character of antiferromagnetically ordered magnetic electrons [16].When A^{3+} is also magnetic, normally a lanthanide cation, the magnetic behavior is the result of the contributions given by the two different magnetic A_4 and B_4 tetrahedral networks. However, in most of the lanthanide iridium pyrochlores it is possible to observe, by magnetic susceptibility measurements, a transition that suggests a spin-glass magnetic behavior [10,17].

When electrical properties are considered, iridium pyrochlores exhibit a wide variety of electrical responses that could fall either into the metallic conductivity regime or into a Mott–Hubbard electron localization-type phenomenon [10,17] the iridium pyrochlores, since it modifies the Ir–O1 distance, that is, the overlap between oxygen 2*p* and iridium 5*d* orbitals [18]. In this paper, the synthesis and structural analysis of the $Bi_{2-y}Sr_yIr_2O_7$ α-pyrochlore solid solution are reported. The motivation of this work is the possibility of providing a system in which the correlation between structural parameters and the electrical and magnetic behavior could be established [19]. Here, the relationship between crystal structure changes in $Bi_{2-y}Sr_yIr_2O_7$ and electrical properties is showed. The pyrochlore crystal structure is especially stable and even under high-pressure conditions no structural phase transitions have been found in $A_2B_2O_7$ (A=Tb, B=Ti, Sn, and Mo) [20] and some effects of compression can be achieved with chemical substitution. The main effects associated with mechanical or chemical modification on pyrochlores, that are expected to change their electronics properties, are those that modify the *B*–*B* bond distance (especially when *B* is magnetic) and the *B*–O–*B* bond angle. Small changes in the crystal structure, associated with the cation substitution, are important because the potential magnetic and electrical applications are associated with them [16,17]

2. Experimental details

Fine powder of iridium oxide (IrO_2, 99.9%), bismuth oxide (Bi_2O_3, 99.99%) and strontium carbonate ($SrCO_3$, 99.995%) were used in the solid-state chemical reaction to obtain ten compositions of the $Bi_{2-y}Sr_yIr_2O_7$ system ($0.0 \le y \le 0.9$). Pellets of these chemicals were made from an intimate stoichiometric mixture of the components by compaction at 1 GPa using a 5 mm-steel die. These compounds were synthesized by heating the pellets at 873, 1073 and 1323 K for 12, 24 and 48 h in air, respectively, with intermediate regrindings. A special care should be taken with the second temperature of this synthesis route, since it is close to the melting temperature for Bi_2O_3 and phase segregation may occur. The single-phase formation of these compounds was confirmed by X-ray diffraction (*XRD*) of powders. Synthesis under oxygen atmosphere was also tried, but for the $y \ge 0.7$ compositions, an unidentified additional phase was present.

The crystal structure of these compounds was analyzed from *XRD* data gathered in the 2θ range from 2° to 90°, with $\Delta 2\theta$ step scan of 0.02° and a counting time of 11 s per step. Intensity data were collected at room temperature with a Siemens *D*-5000 X-ray diffractometer (Cu$K\alpha_1$ radiation, $\lambda = 1.5406$ Å) in the transmission mode (Debye–Scherrer geometry) and operating conditions of 35 kV and 35 mA. Identification of the synthesized phases was made using the reference database of the International Centre for Diffraction Data (*ICDD PDF*-2). Initial analyses were made by checking the permitted *hkl*-reflections for the $Fd\bar{3}m$ space group using the *Celref* package [21]; by this procedure the unit cell parameter, peak heights and Miller's indices were initially estimated. Rietveld analyses were performed using the General Structure Analysis System [22] (*GSAS package*) code with the graphical user interface EXPGUI [23]. One Shifted Chebyschev function with ten terms was required to describe the experimental diffraction pattern background. Simulation of X-ray diffraction peaks was carried out with a pseudo-Voigt (*FCJ* Asym) as the profile function [22].

3. Results and discussion

X-ray patterns of the $Bi_{2-y}Sr_yIr_2O_7$ solid solution in the $0.0 \leq y \leq 0.9$ range are shown in Fig. 2.

Due to the small amount of sample, the transmission (Debye–Scherrer) geometry was chosen as the diffraction technique to refine the crystal structure of $Bi_{2-y}Sr_yIr_2O_7$. In this geometry, the diffraction patterns should be corrected for absorption, especially for systems containing heavy atoms as the ones studied here. The transmission geometry is not the best approach for data collection since the strong absorption of the samples for Cu$K\alpha$ radiation would require a precise absorption correction of data before a Rietveld analysis is performed [24]. In the case of the Rietveld refinement, inaccurate absorption corrections will result in unrealistic values of thermal vibration parameters [24]. Using the Cu$K\alpha_1$ radiation in the reflection geometry (Bragg–Brentano), since none of the direct beam passes through the sample, no absorption correction is needed during analysis of the diffracted intensities and the reflection geometry is the adequate mode to prevent such problem [25]. In spite of a reduction in the intensity of reflections, especially at low scattering angles, a careful arrangement of powders by trapping the sample between two layers of a thin film (Mylar, 6 μm), was judged adequate to proceed with no correction factor, expecting only low values in the goodness of fit (χ^2) criteria. By this procedure, changes in sample absorption as a function of diffraction angle can be neglected in symmetrical flat plane geometry, contrary as in a capillary tube array occurs [26].

Data of the polycrystalline compounds were refined with a α-pyrochlore structure model, with A=(Bi, Sr) atoms on 16*d* site (½, ½, ½); Ir on 16*c* site (0, 0, 0); O1 on 48*f* site (x, $^1/_8$, $^1/_8$), and O2 on 8*b* site ($^3/_8$, $^3/_8$, $^3/_8$), Fig. 1 (in this figure the positions are shifted by ½, ½, ½ for viewing purposes). For the Rietveld refinements, the atomic coordinates given by Kennedy [27] for $Bi_2Ir_2O_7$ were taken as the starting model. After that, atomic positions, occupations and other structural parameters were extracted in order to investigate more closely the changes in the crystal structure of $Bi_{2-y}Sr_yIr_2O_7$ and these results are summarized in Table 1. A sample of the Rietveld refinement results, in a graphic mode, is showed for the upper limit of solubility of Sr, $Bi_{1.1}Sr_{0.9}Ir_2O_7$, in Fig. 3.

From the Rietveld analyses of samples of the solid solution, a regular increase of the cubic lattice parameter as a function of the Sr content can be observed, see Fig. 4. This change in the cell parameter is due to the steric effects provoked by the ionic radii of cations (Vegard's law), since Sr^{2+} is bigger than Bi^{3+}, (Bi^{3+} = 1.31 Å, Sr^{2+} = 1.40 Å) [28].

In order to analyze whether the Bi substitution by Sr modifies the α-pyrochlore structure of $Bi_{2-y}Sr_yIr_2O_7$ towards an oxygen-defective fluorite structure, the O1 position was studied. In the ideal α-pyrochlore structure, the oxygen atoms are not equivalent, all of them have tetrahedral coordination, but the O1 atoms are surrounded by two Bi (Sr) and two Ir cations, whereas the O2 atoms are surrounded by four Bi (Sr) cations. Due to symmetry,

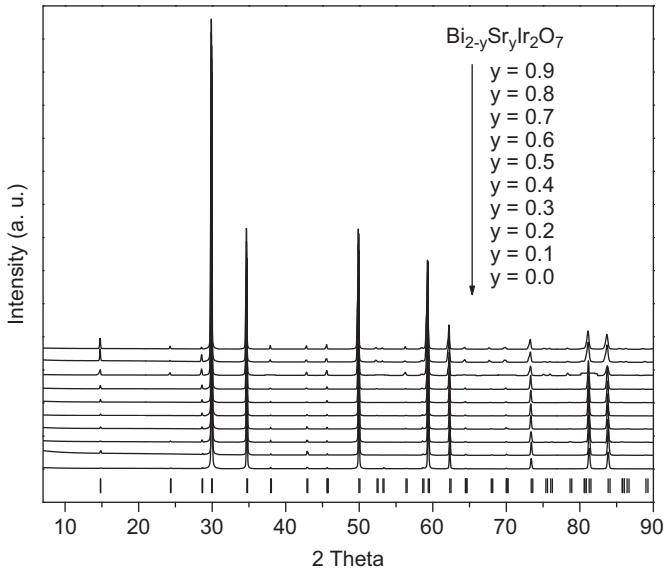

Fig. 2. X-ray diffraction patterns for the $Bi_{2-y}Sr_yIr_2O_7$ system. The intensities were normalized to one for visual purposes. Pyrochlore Bragg reflections are shown at the bottom of the graph.

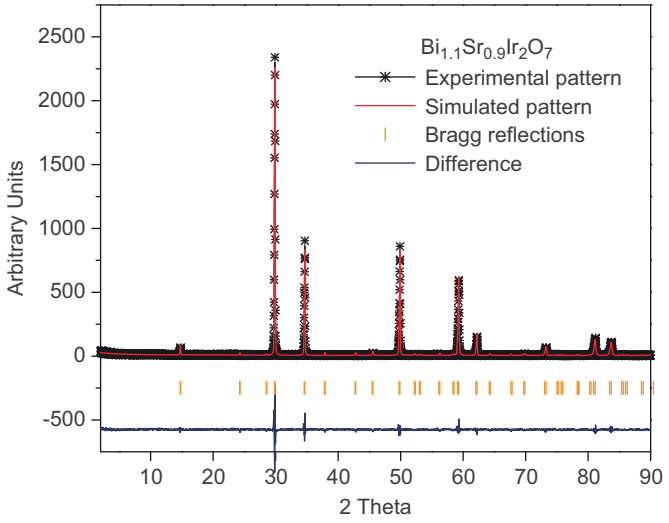

Fig. 3. Rietveld refinement results for the $Bi_{1.1}Sr_{0.9}Ir_2O_7$ sample.

Table 1
Rietveld refinement results and crystal-cell parameters of the $Bi_{2-y}Sr_yIr_2O_7$ solid solution.

Composition y	χ^2	Cell parameter (Å)	Position of O1	Occupation of Ir	Occupation of O1	Occupation of O2
0.0	4.15	10.3121 (3)	0.3314 (1)	0.91 (1)	0.98 (6)	1.00
0.1	3.94	10.3132 (2)	0.3280 (1)	0.94 (2)	0.92 (1)	0.91 (2)
0.2	4.78	10.3159 (2)	0.3246 (2)	0.97 (1)	0.96 (2)	0.82 (2)
0.3	4.87	10.3199 (1)	0.3204 (1)	0.98 (3)	0.90 (2)	0.96 (1)
0.4	4.17	10.3219 (2)	0.3161 (4)	0.96 (1)	0.97 (8)	0.97 (1)
0.5	4.30	10.3221 (3)	0.3133 (1)	0.97 (1)	0.94 (5)	0.93 (2)
0.6	2.47	10.3240 (1)	0.3090 (2)	0.99 (1)	0.95 (9)	0.94 (1)
0.7	3.15	10.3255 (3)	0.3040 (1)	0.91 (2)	0.94 (4)	0.99 (1)
0.8	3.17	10.3283 (2)	0.2996 (2)	0.99 (1)	0.98 (1)	0.96 (2)
0.9	2.87	10.3318 (4)	0.2972 (3)	0.94 (6)	0.94 (4)	0.89 (1)

[†]Atomic occupations of Bi -or Sr- were not refined.

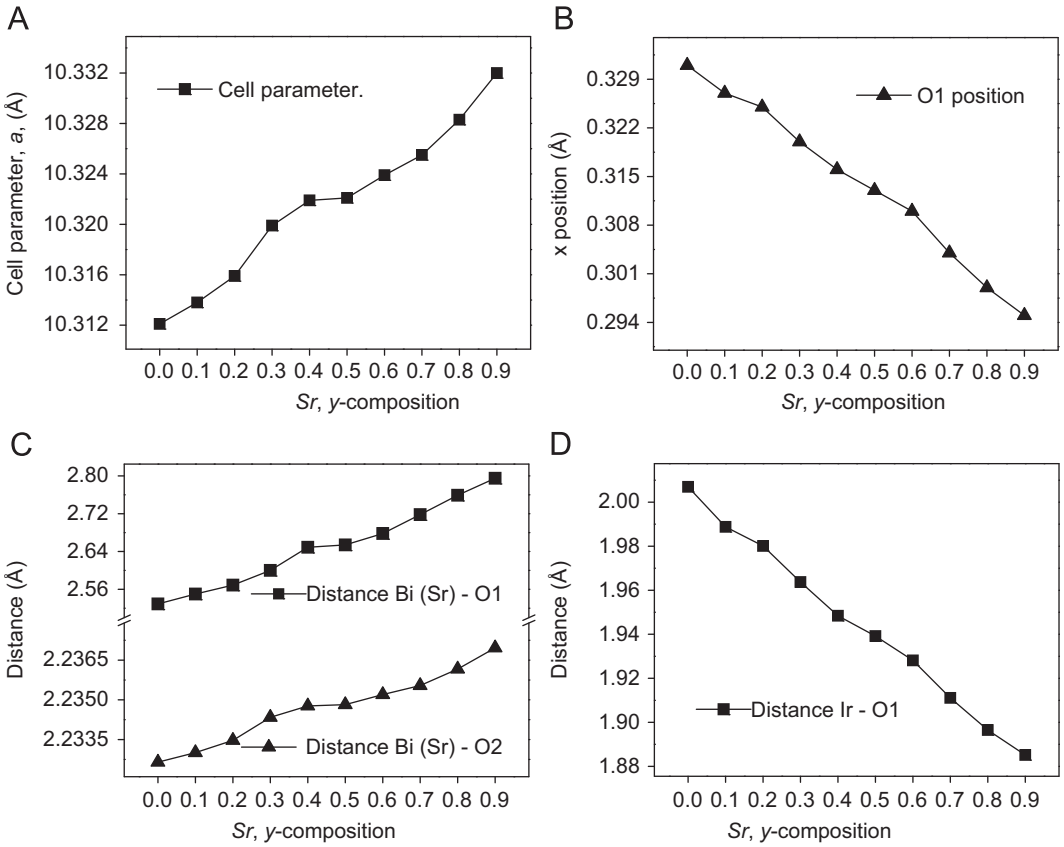

Fig. 4. (A) Crystalline parameter values of $Bi_{2-y}Sr_yIr_2O_7$; (B) *x*-coordinate of O1; (C) Bi(Sr)-O1 and Bi(Sr)-O2 distances; and (D) Ir–O1 distance, all of them plotted as a function of the *y*-composition.

the O2 are equidistant from all their coordination-cations. On the other hand, the coordination-distances of the O1 are not equal, since the oxygen is closer to the Ir cations [29–31]. In the defect fluorite structure, the O1 is in $x=0.375$ and all distances between the O1 and the two types of cations are equal. In this work, it has been observed, after Rietveld analysis, that the position of O1 changes smoothly, see Fig. 4, and its mean value is $x=0.314\pm0.0011$ Å. This value lies into the limit 0.3125–0.375, which corresponds with a α-pyrochlore structure and not with a defect fluorite-type structure. Due to the high symmetry of O2, its position is not affected by the Sr substitution.

As expected for an aliovalent substitution in solid solutions, here Sr^{2+} by Bi^{3+} in $Bi_{2-y}Sr_yIr_2O_7$, an increase in the valence state of Ir or Bi was reasonably anticipated if the oxygen content is maintained constant. Initial cyclic voltammetric measurements on samples did not reveal the presence of Bi(V) and similarly, Kennedy [14] reports only Bi(III) in $Bi_2Ir_2O_7$. On the other hand, some of Ir(V) has been found by magnetization measurements only in the $y=0.0$ sample [19] The existence of Ir(V), coexisting with Ir(IV) in the surface of $Pb_2Ir_2O_7$, has previously been suggested on the basis of different Ir–O bond distances [14].

From the results of the Rietveld analyses and concerning to the stoichiometry of samples, there are several observations that should be highlighted. With regard to the Ir occupation, it should be pointed out that the prolonged time of the solid-state reaction to obtain $Bi_{2-y}Sr_yIr_2O_7$ could lead to evaporation and disproportionation of the iridium-oxide, releasing oxygen [13]. In the synthesis method to obtain $Bi_{2-y}Sr_yIr_2O_7$, no additional amounts of IrO_2 were used in order to compensate these losses and this could be the reason because the Ir occupation is low with respect to the nominal composition. Even though the Bi substitution by Sr, due to charge balance considerations could lead to the formation of Ir(V), this condition is not valid due to the oxygen loss during the high temperature reaction. According to the charge balance fitting, from the O1 and O2 occupation in the refinement results, a Ir(IV)–Ir(V) mixture is present in $Bi_{2-y}Sr_yIr_2O_7$ for $y=0.0$, 0.4, 0.7, 0.8 and 0.9. This result is consistent with the number of Bohr magnetons (μ_B) that have been observed, 1.35 μ_B, for the $y=0.0$ sample [Ir^{4+} (d^5) has $\mu_{eff}=1.73$ μ_B; Ir^{5+}, with a singlet ground state in a distorted octahedral crystal field splitting is non-magnetic at low temperatures] [32]. The magnetic behavior for the $y>0.0$ samples do not follow a Curie–Weiss law and the values of μ_B deserves an additional discussion [19]. On the other hand, the occupation results of the refinement suggest that for $y=0.1$, 0.2, 0.3, 0.5 and 0.6 an Ir(IV)–Ir(III) mixture is present. These irregularities in the Ir and O occupation are due probably to the synthesis route for these compounds, since for IrO_2 in the temperature range above 953 K, dissociation to Ir and O_2 occurs [33].

Apart from the loss of oxygen that occurs during the chemical reaction to produce the solid solution $Bi_{2-y}Sr_yIr_2O_7$, there is an additional factor accounting for the results on O1 and O2 SOF's of the Rietveld refinement results. This is related to the oxygen anions that are located in several planes occupied by heavy atoms (Bi and Ir, particularly in 113 and 226 for O1, and 224 for O2). In such situation, their scattering is expected to be diminished; in this case, the O occupation determination by means of X-ray powder diffraction is not reliable. Neutron diffraction becomes necessary to accurately determine the O1 and O2 occupations in these compounds.

The O1 movement results as a function of the Sr content are consistent with the theoretical structural properties suggested by Koo et al. [18]. Accordingly, in any tetrahedron (FCC and spinel structure included), as those present in the pyrochlore structure (Bi_2Ir_2O), a bigger *A* cation repels more strongly the O1 atom than

Table 2
Angle and distance values for ten compounds of the solid solution $Bi_{2-y}Sr_yIr_2O_7$ ($0.0 \le y \le 0.9$).

Composition y	Ir–O1	Distance (Å)		Bond angle (deg)	
		Bi–O1	Bi–O2	Ir–O1–Ir	O1–Ir–O1′[a]
0.0	2.00696 (5)	2.519 (2)	2.23265 (6)	130.54 (1)	82.83 (1)
0.1	1.99276 (7)	2.543 (1)	2.23287 (7)	132.37 (1)	84.03 (2)
0.2	1.97954 (5)	2.568 (2)	2.23347 (6)	134.21 (2)	85.26 (4)
0.3	1.96373 (4)	2.600 (3)	2.23434 (2)	136.56 (1)	86.86 (1)
0.4	1.94839 (2)	2.632 (3)	2.23477 (2)	138.94 (0)	88.51 (6)
0.5	1.93819 (2)	2.654 (2)	2.23482 (6)	140.59 (3)	89.67 (2)
0.6	1.92500 (1)	2.680 (2)	2.23521 (2)	142.90 (4)	91.30 (5)
0.7	1.91110 (1)	2.718 (1)	2.23554 (1)	145.52 (3)	93.57 (1)
0.8	1.89650 (2)	2.759 (4)	2.23616 (8)	148.61 (1)	95.46 (3)
0.9	1.89063 (1)	2.778 (4)	2.23691 (1)	150.05 (1)	96.52 (3)

[a] O1 and O1′ belong to different tetrahedra (Fig. 1B).

a smaller *A* cation. In the present work, it was possible to observe that when Bi^{3+} is substituted by a bigger cation as Sr^{2+}, the O1 moves closer to the Ir cations, see Table 2 and Fig. 4d. This Ir–O distance reduction follows the Sr nominal composition of $Bi_{2-y}Sr_yIr_2O_7$.

4. Electrical properties

Electrical resistivities of samples show a metallic behavior ($d\rho/dT$ positive), Fig. 6. This slope increases with the strontium content of samples, and no metal–insulator transition was observed with the increase of the Sr content. It is worth commenting that both the resistivity and slope of the resistivity increase with Sr content. This could be explained in terms of two elements contributing to the electrical resistivity, see Eq. (1).

To analyze these properties two compositions were calculated; $Bi_2Ir_2O_7$ ($y=0.0$) and $BiSrIr_2O_7$ ($y=1.0$). The cell parameters for the latter were extrapolated from the data in Table 1. The Density of States (DOS) for these compounds are shown in Fig. 5, at the Fermi energy, E_F, they have the same total value.

The electrical conductivity ($\sigma_\alpha = 1/\rho_\alpha$, in the α direction, where ρ is the resistivity) in the relaxation time approximation, is [34,35]

$$\sigma_\alpha = (e^2/\hbar\Omega)\tau \int v_\alpha dA_\alpha \quad (1)$$

where v_α is the electron velocity ($=d\varepsilon/dk_\alpha$), A_α is the area perpendicular to v_α, the integral is evaluated at E_F, and τ is the relaxation time which depends on the 'imperfections' of the crystal. The integral of Eq. (1) contains terms that are related to the electronic structure of the crystal, these terms show a modest increase (19%) when Bi is replaced by Sr. The increase of the resistivity is due to the scattering of the imperfections in the crystal, these are due to (a) the replacement of Bi by Sr, in which Sr replaces Bi at random, and (b) Sr^{2+} has a weaker bond than Bi^{3+}, thus it has larger oscillations. These two terms affect the conductivity (Eq. (1)) through the relaxation time τ. τ has two terms that contribute in the following way [35];

$$1/\tau = 1/\tau_d + 1/\tau_{ph} \quad (2)$$

As can be observed from Fig. 5a, in $Bi_2Ir_2O_7$ there are two DOS branches appearing from -2 to -0.7, and from -0.6 to 0.8. With the Sr substitution in $BiSrIr_2O_7$, these broaden and the gap disappears, at some composition with this broadening, more states would become available at E_F. The 19% increase in the electronic part of the conductivity (the integral in Eq. (1)) is due to this broadening.

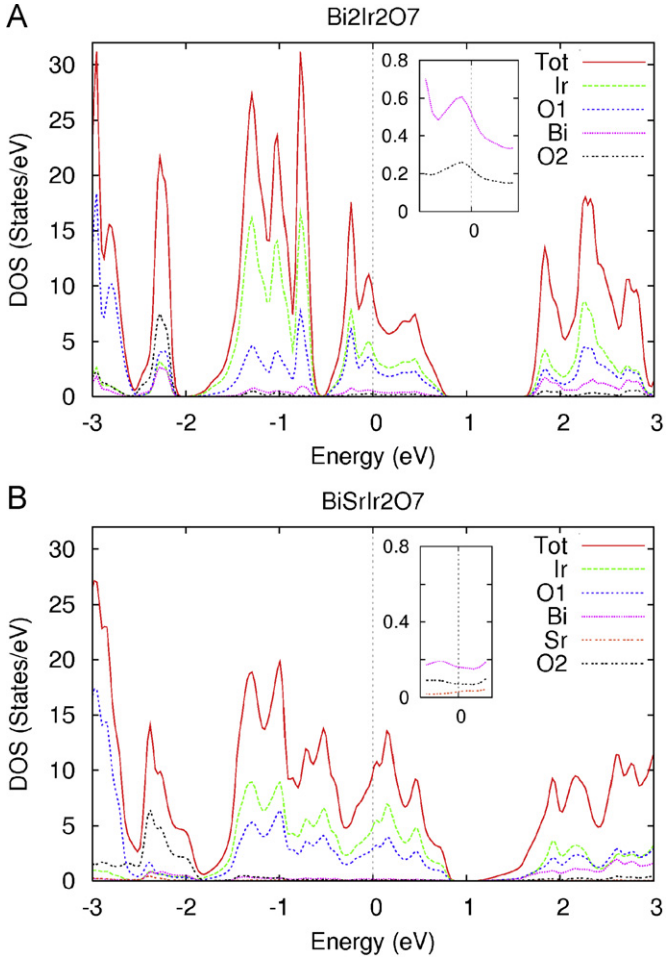

Fig. 5. Density of states for (A) $Bi_2Ir_2O_7$ and (B) $BiSrIr_2O_7$ pyrochlore systems. From these plots a metallic character of both systems can be observed. The main contribution at E_F is from the Ir_2O_6 sublattice, Bi_2O contributes very little. At E_F the total DOS values remain almost constant. The inset shows the Bi, Sr and O2 contributions at E_F.

In Eq. (2), τ_d is due to disorder, which in this case is mainly introduced by Sr that occupies the same crystalline position of Bi but in a random way, therefore with the introduction of Sr the scattering becomes more frequent, which implies that $1/\tau_d$ increases. τ_{ph} is the phononic term due to the oscillations of the atoms, these increase with temperature and $1/\tau_{ph}$ increases. With the introduction of Sr^{2+}, which has a weaker bond than Bi, and it

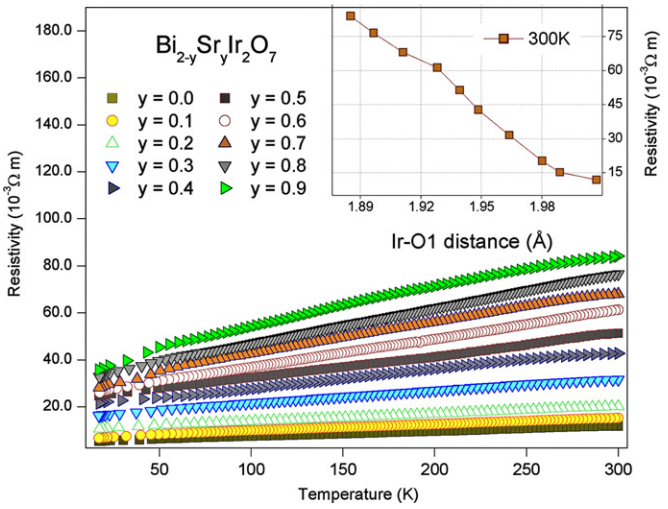

Fig. 6. Temperature dependence of resistivity for $Bi_{2-y}Sr_yIr_2O_7$. Inset shows resistivity change in function of Ir–O1 distance at 300 K.

should have larger oscillations; therefore the temperature dependence of $1/\tau_{ph}$ should increase.

As mentioned above the electronic term has a small effect increasing the conductivity, or reducing the resistivity. On the other hand the scattering terms have a much larger increment with Bi replacement by Sr.

5. Conclusions

In the present work it was shown that it is possible to obtain single-phase $Bi_{2-y}Sr_yIr_2O_7$ compounds in the $0.0 \leq y \leq 0.9$ range, all of them with α-pyrochlore-type cell. With the use of X-ray Rietveld analysis it is possible to observe that the movement of the O1 plays a special role because it is the connector between the Bi_2O and the Ir_2O_6 networks. With the substitution of Bi^{3+} by the larger Sr^{2+} cation, this O1 moves away from this cation and moves closer to Ir. With this substitution the electronic structure part of the conductivity, due to the shortening in the Ir–O1 bond, shows a moderate increase (19%). On the other hand the static and dynamic imperfections of the crystal structure shorten the relaxation time and the net resistivity and its temperature dependence increases with the Sr^{2+} content.

Acknowledgment

We thank Cecilia Salcedo, of USAI laboratories in Facultad de Química UNAM, for valuable help in X-ray diffraction measurements. This work was done with support from DGAPA-UNAM under project PAPIIT IN105207-3.

References

[1] F.E. Osterloh, Chemistry of Materials 20 (2008) 35.
[2] F.X. Zhang, J.W. Wang, J. Lian, M.K. Lang, U. Becker, R.C. Ewing, Physical Review Letters 100 (2008) 045503.
[3] R.C. Ewing, W.J. Weber, J. Lian, Journal of Applied Physics 95 (2004) 5949.
[4] B.I. Omel'yanenko, T.S. Livshits, S.V. Yudntsev, B.S. Nikonov, Geology of Ore Deposits 49 (2007) 173.
[5] S.V. Stefanovsky, S.V. Yudintsev, R. Gieré, G.R. Lumpkin, The Geological Society of London 236 (2004) 37.
[6] T. Konishi, H. Kawai, M. Saito, J. Kuwano, H. Shiroishi, T. Okumura, Y. Uchimoto, Topics in Catalysis 52 (2009) 896.
[7] A.P. Ramirez, Annual Review of Materials Science 24 (1994) 453.
[8] J.S. Gardner, M.J.P. Gingras, J.E. Greedan, Reviews of Modern Physics 82 (2010) 53.
[9] M. Hanawa, Y. Muraoka, T. Tayama, T. Sakakibara, J. Yamura, Z. Hiroi, Physical Review Letters 87 (2001) 187001.
[10] D. Yanagishima, Y. Maeno, Journal of the Physical Society of Japan 70 (2001) 2880.
[11] B.-J. Yang Y.B. Kim, Physical Review B 82, (2010) 085111 and X. Wan, A. Turner, A. Vishwanath, and S.Y. Savrasov, arXiv:1007.0016v1 2010.
[12] M.A. Subramanian, G. Aravamudan, G.V.Subba Rao, Progress in Solid State Chemistry 15 (1983) 55.
[13] D.E. Peterson, Thermodynamics and Transport of Gaseous Iridium Oxide in Multi-Hundred-Watt Thermoelectric Generators. National Technical Information Service, U.S. Department of Commerce, UC-4 & UC-25, May 1976.
[14] B.J. Kennedy, Journal of Solid State Chemistry 123 (1996) 14.
[15] H. Fukazawa, Y. Maeno, Journal of the Physical Society of Japan 71 (2002) 2578.
[16] H. Sakai, H. Ohno, N. Oba, M. Kato, K. Yoshimura, Physica B 329-333 (2003) 1038.
[17] N. Aito, M. Soda, Y. Kobayashi, M. Sato, Journal of the Physical Society of Japan 72 (2003) 1226;
M. Soda, N. Aito, Y. Kurahashi, Y. Kobayashi, M. Sato, Physica B 329-333 (2003) 1071.
[18] H.-J. Koo, M.–H. Whangbo, B.J. Kennedy, Journal of Solid State Chemistry 136 (1998) 269.
[19] C. Cosio-Castaneda et al. in preparation.
[20] A. Apetrei, I. Mirebeau, I. Goncharenko, W.A. Crichton, Journal of Physics: Condensed Matter 19 (2007) 376208.
[21] J. Laugier, B. Bochu, CELREF Program Part of the LMGP Suite of Programs for Windows, Laboroatoire des Materiaux et du Génie Physique de l'Ecole Supérieure de Physique de Grenoble, France, 2000.
[22] A.C. Larson , R.B. Von Dreele, General Structure Analysis System (GSAS), Los Alamos National Laboratory Report LAUR 86-748, 2000.
[23] B. Toby, Journal of Applied Crystallography 34 (2001) 21.
[24] C.R. Ross II, Journal of Applied Crystallography 25 (1992) 628.
[25] W. Pitsche, J.A.L. Collazo, H. Hermann, V.D. Hildebrand, Journal of Applied Crystallography 29 (1996) 561.
[26] R.J. Hill, I.C. Madsen, in: W.I.F. David et al.(Ed.), Structure Determination from Powder Diffraction Data, Oxford University Press, New York, 2002, p. 98.
[27] B.J. Kennedy, Physica B 241-243 (1998) 303.
[28] R. Shannon, Acta Crystallographica A 32 (1976) 751.
[29] B.P. Mandal, A. Banerji, V. Sathe, S.K. Deb, A.K. Tyagi, Journal of Solid State Chemistry 180 (2007) 2643.
[30] W.W. Barker, P.S. White, O. Knop, Canadian Journal of Chemistry 54 (1976) 2316.
[31] G.D. Blundred, C.A. Bridges, M.J. Rosseinsky, Angewandte Chemie International Edition 43 (2004) 3562.
[32] M.W. Lufaso, H.-C. zur Loye, Inorganic Chemsitry 44 (2005) 9143.
[33] Christian Urgeghe, PhD Thesis, Universitá degli Studi di Ferrara, March 2006.
[34] P. de la Mora, M. Castro, G. Tavizon, Journal of Physics: Condensed Matter 17 (2005) 965.
[35] N.W. Ashcroft , N.D. Mermin, Solid State Physics, chapters 13 and 16. Holt-Saunders International Editions, London, 1976.